SAND2021-14986C

Multi-Color Pyrometry of High-speed Ejecta from Pyrotechnic Igniters

Benjamin R. Halls,[1] William E. Swain,[2] Shawn C. Stacy, [3]
Ryan T. Marinis, [4] and Sean P. Kearney[5]
Sandia National Laboratories, Albuquerque, NM, 87122, USA

A high-speed, two-color pyrometer was developed and employed to characterize the temperature of the ejecta from pyrotechnic igniters. The pyrometer used a single objective lens, beamsplitter, and two high-speed cameras to maximize the spatial and temporal resolutions. The pyrometer used the integrated intensity of under-resolved particles to maintain a large region of interest to capture more particles. The spectral response of the pyrometer was determined based on the response of each optical component and the total system was calibrated using a black body source to ensure accurate intensity ratios over the range of interest.

I. Introduction

Energetic devices, such as pyrotechnic hot wire igniters, can release energy in the form of hot gases, hot high-velocity particles, and shock waves. Understanding the role and interplay of the various forms of released energy from such devices is linked to their performance, reliability, and safety [1]. Several methods have been developed to characterized pyrotechnic igniters including measuring heat transfer with thermocouples [2] and shockwave outputs using schlieren [3,4]. These methods help quantify the igniters but do not isolate the contributions of the small (order 10s of microns) hot particles moving at 100s of meters per second. Previous measurements to quantify hot particles and their combustion gases have been developed including planar laser induced fluorescence (PLIF) [5], absolute infra-red (IR) imaging [6], coherent anti-Stokes spectroscopy (CARS) [7], absorption spectroscopy [8], and optical pyrometry [8–11].

This proceeding describes the development of a two-color pyrometer for spatially and temporally under-resolved particles while covering a relatively large region of interest. In place of a pixel-wise temperature measurement, the pixel intensities are integrated to overcome image noise and spatial and temporal blur to yield useful temperature information.

II. Experimental Setup

The imaging setup was composed of the igniter on a three-dimensional translation stage, a single backwards facing 105 mm, f/2 Nikon objective, a Semrock 45 degree longpass imaging beamsplitter with cutoff frequencies at 765 nm, and two Photron SA-Zs with Edmund bandpass filters selected to image the spectral regions of 700 +/- 25 nm and 900 +/- 25 nm. The schematic of the experimental setup is shown in Fig. 1a. The igniter and cameras used a single trigger, and the delay of one camera was adjusted to reduce the jitter between frames to ~40 ns. The cameras were run at 100 kHz with an exposure of 160 ns to collect multiple images of each particle and reduce the temporal blur, respectively. The use of two cameras increased the spatial extent of the images to collect temperature data from as many particles as possible. The image size was 3.7 × 5.5 mm^2 or 312 × 512 pixels with a nominal resolution of 10.8 μm per pixel. The approximate particle size was 35 μm. As such the particles were not well resolved by the imaging system and a

[1] R&D S&E, Mechanical Engineer, AIAA Member.
[2] Test Operations Engineer.
[3] R&D S&E, Mechanical Engineer.
[4] R&D S&E, Mechanical Engineer.
[5] R&D S&E, Mechanical Engineer, AIAA Member.

pixel wise ratio would not be accurate or meaningful. Therefore, the integrated particle intensity was used to determine the intensity ratio and thereby the temperature. To locate the same particle in both images the cameras were registered using a dot card to correlate the images. The imaging system was calibrated using a Mikron 390 blackbody source that varied in temperature from 1270 to 3270 K. The calibration data and fit used to determine the temperature of the particles is shown in Fig. 1b. There is a small discrepancy in the calibration data, and the calibration will need to be repeated for increased accuracy.

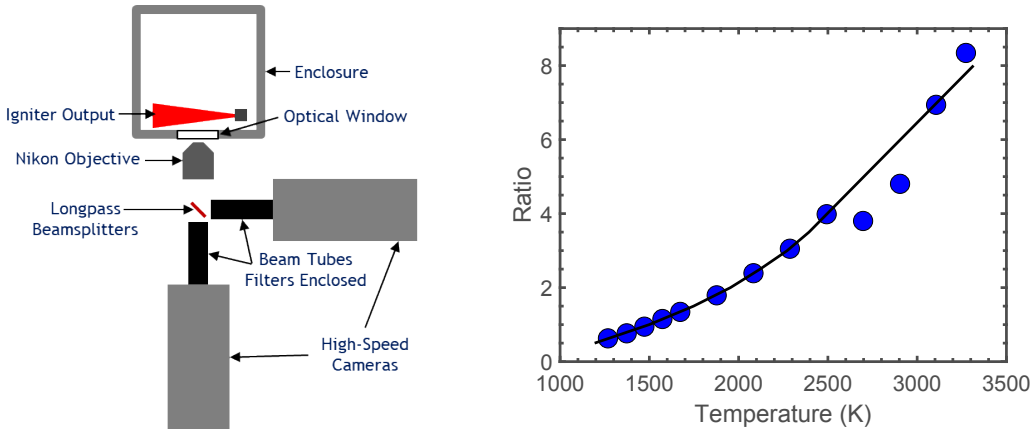

(a) **(b)**

Fig. 1 Experimental setup of the two-color high-speed imaging pyrometer (a) and the blackbody calibration data and curve fit (b).

III. Results and Discussion

Figure 2 shows sample images of the particle field from the igniter at 700 nm (Fig. 2a) and 900 nm (Fig. 2b) and the product of the two images (Fig 2c). The product image increased the contrast of the in-focus particles and provided a single image to locate the particles to reduce the uncertainties of noise, blur, and camera calibration. The high-contrast image was used to locate the particles based on the peak pixel intensities.

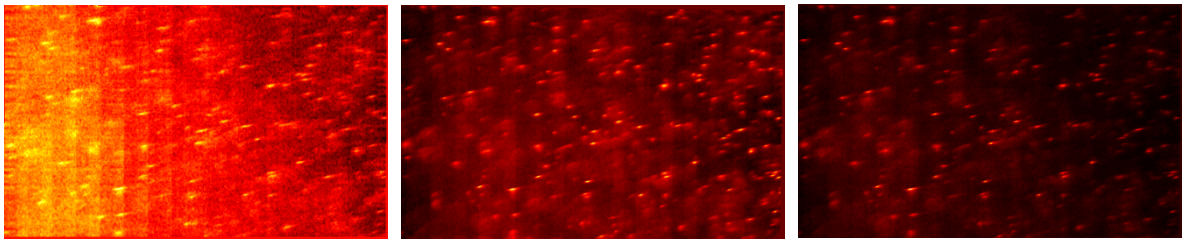

(a) **(b)** **(c)**

Fig. 2 Sample images of the particle field at (a) 700 nm and (b) 900 nm and (c) the product image.

The particle processing routine consisted of several steps to segment and isolate the particles, determine the background intensity, and the integrated intensity ratio for each particle. The routine started by locating the brightest pixel in the product image. Sub images of the 700 nm (Fig. 3a) and 900 nm (Fig. 3b) images were generated around that located pixel, the sub image size was large to fully encompass the largest particles. If the particle located was determined to be at minimum 16 pixels in area the routine continued. An average of the two images (Fig 3c) was generated to make the masks, such that the masks were identical for both the 700 nm and 900 nm sub images. Masks were made to isolate the particle (Fig 3d) and the background (Fig 3e). The contrast was normalized in the averaged image and a relative threshold of 0.4 was applied. The masked areas were enlarged by 2 pixels to encompass the particles. The background mask located other particles in the image and blocked them. Then the background mask was applied to the sub images and they were further cropped (Fig. 3f and 3g top), based on the size of the particle, to determine the local background counts. The background counts were subtracted from the particle sub images, the particle mask was applied and cropped (Figs. 3f and 3g bottom), and the image intensities were integrated. After a particle was located and the intensity ratio determined the particle was masked from the product image and the next

brightest pixel was found and the routine started again. If the particle did not meet the size and contrast criteria, then the area around the peak signal was masked such that the next brightest particle could be found. The potential bias in a process based on choosing the brightest (hottest, largest, or most in-focus) particles first was accounted for by searching for more particles than exist in the images.

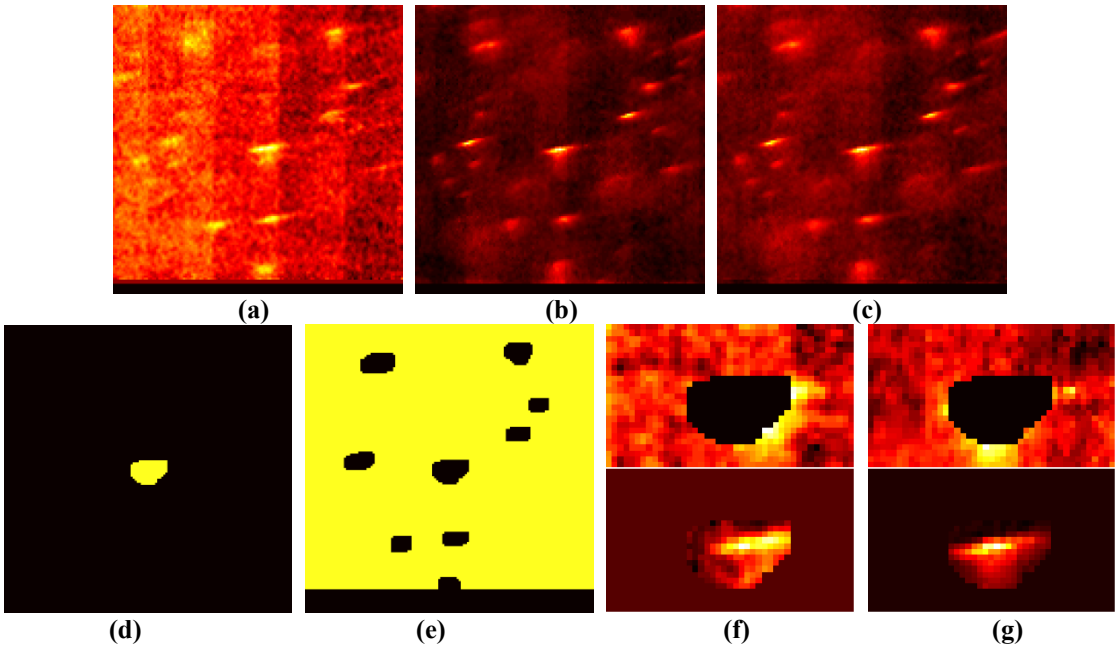

Fig. 3 Sample sub images and masks used in the particle intensity ratio routine: (a) 700 nm sub image, (b) 900 nm sub image, (c) averaged image, (d) particle mask, (e) background mask, (f) cropped and masked sub images of 700 nm background (top) and particle (bottom), (g) cropped and masked sub images of 900 nm background (top) and particle (bottom).

The particle integrated temperature was determined using the measured intensity ratio and the calibration from the blackbody source. The particle's emissivity was assumed to be constant over the spectral range of interest. The particle temperatures were determined for each image in the time sequence provided the located particle met the size and contrast criteria. Figure 4a shows the temperature and standard deviation of the particles located in the image sequence from which the sample images in Fig. 2 were taken at 270 μs. Figure 4b shows the particle count for each image. From this data the particles from the igniter appear to reduce in temperature (2600 to 2300 K) the later they are ejected and arrive within the region of interest. However, more experiments and full understanding of the measurement uncertainties will be required to draw any conclusions.

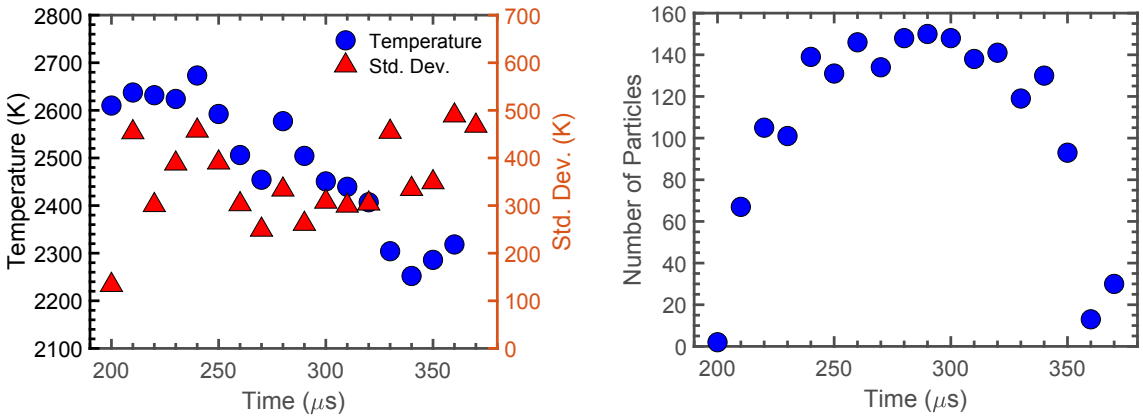

Fig. 4 (a) Time sequence of average particle temperatures and standard deviations, and (b) the time sequence of the number of particles in the region of interest.

IV. Conclusions

A two-color pyrometer was developed to measure the temperature of spatially and temporally under-resolved particles ejected from a pyrotechnic igniter. The method used the integrated intensity of the particles from both images to estimate the temperature and the uncertainty. The pyrometer was calibrated, and preliminary results were shown of a time sequence of particles from an igniter. A full accounting of the measurement uncertainties and more experiments will need to be conducted to define the accuracy and precision of the pyrometer.

Acknowledgments

This paper describes objective technical results and analysis. Any subjective views or opinions that might be expressed in the paper do not necessarily represent the views of the U.S. Department of Energy or the United States Government. Sandia National Laboratories is a multimission laboratory managed and operated by National Technology & Engineering Solutions of Sandia, LLC, a wholly owned subsidiary of Honeywell International Inc., for the U.S. Department of Energy's National Nuclear Security Administration under contract DE-NA0003525. **SAND2021-XXXX**.

References

[1] Cooper, P. W., *Explosives Engineering*, Wiley-VCH, 1996.
[2] Evans, N. A. and Durand, N. A., "Heat transfer characteristics of igniter output plumes," SAND89-0271C, Sandia National Laboratories, Albuquerque, NM 1989.
[3] Skaggs, M. N., Hargather, M. J., and Cooper, M. A., "Characterizing pyrotechnic igniter output with high-speed schlieren imaging," *Shock Waves*, Vol. 27, 2017, pp. 15–25.
[4] Guo, S. and Cooper, M. A., "Multivariate Regression of Pyrotechnic Igniter Output," SAND2020-0416, Sandia National Laboratories, Albuquerque, NM 2020.
[5] Bucher, P., Yetter, R. A., Dryer, F. L., Parr, T. P., and Hanson-Parr, D. M., "PLIF species and radiometric temperature measurements of aluminum particle combustion in O2, CO2, and N2O oxidizers, and comparison with model calculations," *Proc. Combust. Inst.*, Vol. 27, 1998, pp. 2421–2429.
[6] Harrison, J., Brewster, Q., "Infrared emitted intensity measurements from burning aluminum droplets in solid propellants," *Combust. Sci. Technol.*, Vol. 181, No. 1, 2009, pp. 18–35.
[7] Kearney, S. P. and Guildenbecher, D. R., "Temperature measurements in metallized propellant combustion using hybrid fs/ps coherent anti-Stokes Raman scattering," *Appl. Opt.*, Vol. 55, No. 18, 2016, pp. 4958–4966.
[8] Glumac, N., Krier, H., Bazyn, T., Eyer, R., "Temperature measurements of aluminum particles burning in carbon dioxide," *Combust. Sci. Technol.*, Vol. 177, No. 3, 2005, pp. 485–511.
[9] Panagiotou, T., Levendis, Y., and Delichatsios, M., "Measurements of Particle Flame Temperatures Using Three-Color Optical Pyrometry," *Combust. Flame*, Vol. 104, No. 3, 1996, pp. 272–287.
[10] McNesby, K. L., Homan, B. E., Benjamin, R. A., Boyle, V. M., Densmore, J. M., Biss, M. M., "Quantitative imaging of explosives with high-speed cameras," *Rev. Sci. Instrum.*, Vol. 87, 2016, 051301.
[11] Chen, Y., Guildenbecher, D. R., Hoffmeister, K. N. G., Cooper, M. A., Stauffacher, H. L., Oliver, M. S., and Washburn, E. B., "Study of Aluminum Particle Combustion in Solid Propellant Plumes using Digital In-line Holography and Imaging Pyrometry," *Combust. Flame*, Vol. 182C, 2017, pp. 225–237.
[12] Marsh, A. W., Wang, G. T., Heyborne, J. D., Guildenbecher, D. R., and Mazudmar, Y. C., "Time-resolved Size, Velocity, and Temperature Statistics of Aluminum Combustion in Solid Rocket Propellants," Proc. Combust. Inst., 2020.